Feedback-induced destabilization of a laser diode using wavelets

Alejandra Figliola [1] and Cristina Masoller [2]
[1] *Instituto de Cálculo, FCEN, UBA, Buenos Aires, Argentina*
[2] *Instituto de Física, Facultad de Ciencias, Universidad de la República Montevideo, Uruguay*
(Received 2 October 1996; revised manuscript received 17 December 1996)

We analyze the feedback-induced destabilization process of a single-mode laser diode with the wavelet transform (WT). We consider transients following an abrupt switch on of the feedback, for feedback levels strong enough so that the final state of operation of the laser is the coherence-collapsed state. The transient regime involves multiscale interactions that exhibit strong localization in both frequency and time, and we demonstrate that by using the WT we can characterize the transient dynamics and capture the essential features associated with the destabilization process in a relatively simple form. [S1050-2947(97)00905-0]

PACS number(s): 42.55.Px, 05.45.+b, 42.65.Sf

I. INTRODUCTION

It is well known that the optical feedback coming from an external mirror may destabilize a laser diode and cause it to switch from a state of coherent emission (with a linewidth of a few MHz), to the so-called coherence collapsed state (which has a linewidth of several GHz). Even though the phenomenon has attracted a lot of attention over the past few years (see, e.g., [1] and references therein), very little is known about the destabilization process itself, and the study of the transient regime to the coherence-collapsed state is of relevance since in coherent optical communications systems the lasers are commonly subjected to unwanted reflections. The behavior of a single-mode laser diode with optical feedback has been phenomenologically classified into distinct regimes, ranging from weak to strong feedback [2]. For very low feedback levels the external cavity just perturbs the laser mode (regime I), but for higher feedback levels it introduces a series of new modes [called external cavity modes (ECM's)] which have optical frequencies ω that are shifted with respect to the emission frequency of the solitary laser ω_0. In regime II the laser shows noise-induced mode hopping between the ECM's. The rate of mode hopping decreases for increasing feedback, and in regime III the laser operates in the dominant mode, which is the minimum linewidth mode [3]. For increasing feedback levels it has been demonstrated that the ECM's undergo a quasiperiodic route to chaos, and that the two frequencies that appear in the route are the relaxation oscillation frequency of the solitary laser f_{ro}, and the external cavity frequency $f_{\mathrm{ext}}=1/\tau$ ($\tau=L_{\mathrm{ext}}/2c$ being the round-trip time in the external cavity of length L_{ext}) [4,5]. In regime IV coherence collapse arises and the laser switches between the chaotic attractors introduced by the ECM's [6]. These attractors have mean optical frequencies that are shifted with respect to ω_0, and since f_{ro} and f_{ext} appear in the route of all the modes, the power spectra of the stationary output of the laser will show peaks at the harmonics of f_{ro} and f_{ext}, either if the laser is operating in a single attractor or if it is switching between several attractors. For even stronger feedback, single-mode narrow linewidth operation is achieved again (regime V).

In this paper we study the transient regime from the coherent emission state of the solitary laser to the coherence collapsed state, using the wavelet transform (WT).

The WT has recently emerged as an important mathematical framework to deal with nonstationary signals [7–9]. Both Fourier transform (FT) and WT can be viewed as a rotation from the time domain to a different domain. For the FT the basis functions are sines and cosines, while for the WT the basis functions are more complicated functions called wavelets. A wavelet is a smooth and rapidly vanishing oscillating function with a good localization both in frequency and in time. Because of the multiresolution analysis that performs, the WT is highly suitable to the analysis of data series containing pulses or short-lived events, since it avoids averaging them when examining large sections of the data.

The transient dynamics to the coherence collapsed state has two very different time scales (the relaxation period and the time delay) and also has time-localized events (the jumps between the attractors introduced by the ECM's). Our purpose is to show that the WT is an excellent technique for the study of the transient regime of the laser, which has not, to our knowledge, been applied before. It permits us to determine which frequencies appear in the transient regime of the laser and to study how their energy distribution evolves in time. Also, from the wavelet coefficients we can calculate the information cost function (ICF) [8] and quantify the increase of the disorder in the transient regime.

This paper is organized as follows. In Sec. II we describe the theoretical model employed and the main characteristics of the dynamics of the laser in the coherence-collapsed regime. Section III presents the results of applying the wavelet transform to the dynamics. The time series of the output intensity and the phase delay in the external cavity are analyzed. Finally, Sec. IV contains our conclusions.

II. THEORETICAL MODEL

We have numerically simulated the dynamics based in the Lang-Kobayashi model [10]. The equations are the usual laser equations plus a time-delayed term that takes into account the field reflected from the external mirror. Writing the intracavity complex field as $E(t)\exp[i\omega_0 t+\phi(t)]$, where ω_0 is the laser frequency in the absence of feedback, the equations read

 © 1997 The American Physical Society

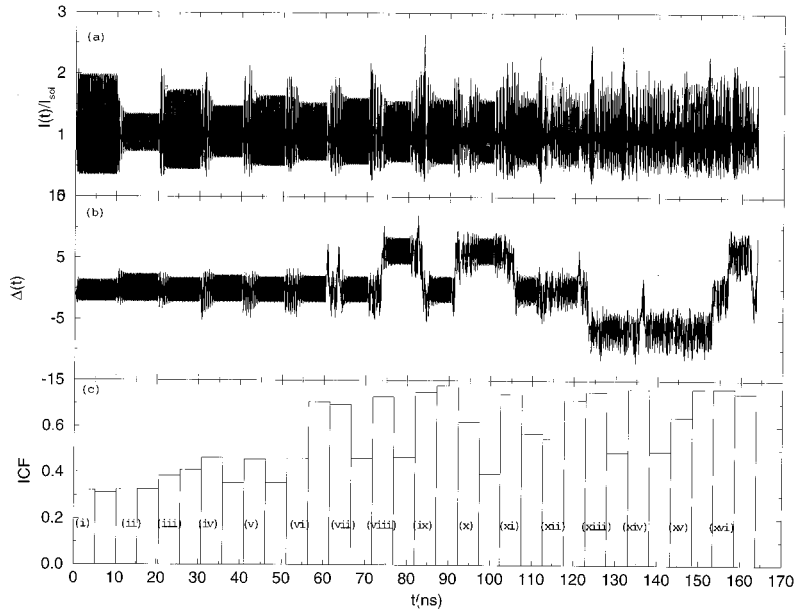

FIG. 1. Simulated time evolution of (a) normalized intensity and (b) phase delay. (c) Time evolution of the ICF, calculated by sliding a 512-data-set window along the series of $\Delta(t)$.

$$\frac{dE(t)}{dt}=\frac{1}{2}\left(G-\frac{1}{\tau_p}\right)E(t)+\gamma E(t-\tau)\cos[\Delta(t)+\omega_0\tau]+\frac{R}{2VE(t)}, \quad (1)$$

$$\frac{d\phi(t)}{dt}=\frac{\alpha}{2}\left(G-\frac{1}{\tau_p}\right)-\frac{E(t-\tau)}{E(t)}\gamma\sin[\Delta(t)+\omega_0\tau], \quad (2)$$

$$\frac{dN(t)}{dt}=J-\frac{N(t)}{\tau_s}-GE(t)^2. \quad (3)$$

In these equations $N(t)$ is the carrier density inside the active region, and the modulus of the electric field $E(t)$ is normalized such that $I(t)=VE(t)^2$ is the total photon number in the laser waveguide, where V is the volume of the active region. τ_s is the carrier lifetime, τ_p is the photon lifetime, and $\tau=2L_{\rm ext}/c$ is the round-trip time of the light in the external cavity of length $L_{\rm ext}$. $\Delta(t)=\phi(t)-\phi(t-\tau)$ is the phase delay in the external cavity. The optical gain is $G=G_N(N-N_0)(1-\epsilon E^2)$, where G_N is the modal gain coefficient, N_0 the carrier density at transparency, and ϵ the gain saturation coefficient. γ is the feedback parameter that measures the intensity of the light reflected from the external mirror. α is the linewidth enhancement factor, J is the current density in carrier per unit volume and unit time, and R is the rate of spontaneous emission into the lasing mode.

The Lang-Kobayashi model is valid for weak to moderated feedback levels (regimes I–IV) since the equations contain a single time-delayed term that takes into account the field fed back into the laser cavity (i.e., multiple reflections are neglected). The spectral and stability properties, and the onset of coherence collapse, have been accurately reproduced by this model [11–13].

The equations were integrated with a fourth-order Runge-Kutta method with a time increment $\Delta t=0.01$ ns. The delay term of Eqs. 1 and 2 requires that the values of $E(t)$ and $\phi(t)$ in a round-trip time are stored in memory and reused in the next round-trip interval. In our numerical simulations the initial conditions were set accordingly to the steady state of the solitary laser, and in $t=0$ the feedback was switched on. The calculations were carried out for an external cavity of 1.5 m ($\tau=10$ ns) and a bias current 100% above threshold. The feedback parameter γ is the free parameter of our study. The laser parameters are as in Ref. [13]: $\tau_s=1$ ns, $\tau_p=1.4$ ps, $\omega_0\tau=6$ rad, $G_N=8.39\times10^{-13}$ m^3 s^{-1}, $N_0=1.23\times10^{24}$ m^{-3}, $\epsilon=2\times10^{-24}$ m^3, $\alpha=4.4$, $V=1.2\times10^{-16}$ m^3, and $R=1.1\times10^{12}$ s^{-1}. For these parameters $f_{\rm ro}=6.65$ GHz and $f_{\rm ext}=0.1$ GHz.

Figure 1(a) shows the time evolution of the normalized light intensity $I(t)/I_{\rm sol}$ ($I_{\rm sol}$ being the intensity of the solitary laser), and Fig. 1(b) shows the time evolution of the phase delay in the external cavity $\Delta(t)=\phi(t)-\phi(t-\tau)$, for $\gamma=4.8$ GHz. Since the instantaneous optical frequency is $\omega=d\phi/dt$, $\Delta(t)/\tau$ is the value of ω averaged a round-trip time.

We know from Ref. [13] that for $\gamma=4.8$ GHz the final state of operation is the coherence-collapsed regime. In Ref. [13] the laser visibility (which is the modulus of the autocorrelation function of the complex electric field) was computed based in the Lang-Kobayashi model, and a good agreement with the experimentally measured visibility was found (our parameters correspond to those of Fig. 4(d) of [13]).

In Fig. 1(a) the jumps between the chaotic attractors introduced by the ECM's cannot be resolved, and at the end of the transient the light intensity is observed to fluctuate seemingly randomly. However, Fig. 1(b) demonstrates that during the first 60 ns the laser remains in the vicinity of the solitary laser mode, but at about $t\approx60$ ns a transition occurs and the laser jumps to another mode (notice the shift in the value of Δ which reveals that the laser jumps to an ECM that has $\omega>\omega_0$). For $t>60$ ns the laser jumps randomly between the chaotic attractors originated from the ECM.

During the destabilization process the laser undergoes intervals of regular oscillations followed by drops of irregular oscillations. Initially the oscillations are the undamped relaxation oscillations and the drops occur with a period almost equal to τ. The time of the first transition and the frequency

of the jumps depend on the feedback level. Decreasing γ increases the time interval in which the laser remains in the solitary laser mode and also increases the time intervals in which the laser operates in a single attractor.

III. WAVELET TRANSFORM

Let us now show the results of analyzing the transient dynamics with the discrete wavelet transform (DWT).

The DWT of a signal $x(t)$ is a set of coefficients $c_{j,k}$ called wavelet coefficients, which are obtained by the decomposition of $x(t)$ onto a basis of functions $\psi_{j,k}$ [7]:

$$c_{j,k}=\langle x(t),\psi_{j,k}(t)\rangle. \tag{4}$$

The functions $\psi_{j,k}$ are obtained from dilations and translations of a single function ψ called the analyzing wavelet. In this work we have chosen a cubic B-spline wavelet basis (to see how these wavelets look like in the time and frequency domains see, e.g., Fig. 1 of Ref. [14]). We have used the Mallat algorithm [7] to compute nearly 2^{-j} wavelet coefficients for each $j=-1,\ldots,-|\ln N|$.

Discrete wavelet analysis breaks down a signal into successive logarithmic frequency bands. The time series shown in Fig. 1 consists of $N=16\,384$ data points sampled with $\Delta t=0.01$ ns. Therefore, the WT decomposes the signal into 15 wavelet bands, the band $j=-1$ represents the signal frequency band 25–50 GHz, $j=-2$ the band 12.5–25 GHz, $j=-3$ the band 6.25–12.5 GHz, etc.

Since the wavelet basis is orthonormal,

$$\langle x(t)^2\rangle \propto \sum_j \sum_k |c_{j,k}|^2, \tag{5}$$

the energy associated with the level j (or scalogram) is

$$\epsilon_j=\sum_k |c_{j,k}|^2. \tag{6}$$

The normalized scalogram π_j is the percentile of energy of the level j, i.e.,

$$\pi_j=\epsilon_j/\sum_j \epsilon_j. \tag{7}$$

Clearly, in the normalized scalogram of the time series of $I(t)/I_{\rm sol}$ [shown in Fig. 2(a)] the major part of the energy is in the wavelet band $j=-3$ (this is the band that contains $f_{\rm ro}$). The rest of the energy is in the neighboring bands $j=-4$ and $j=-2$.

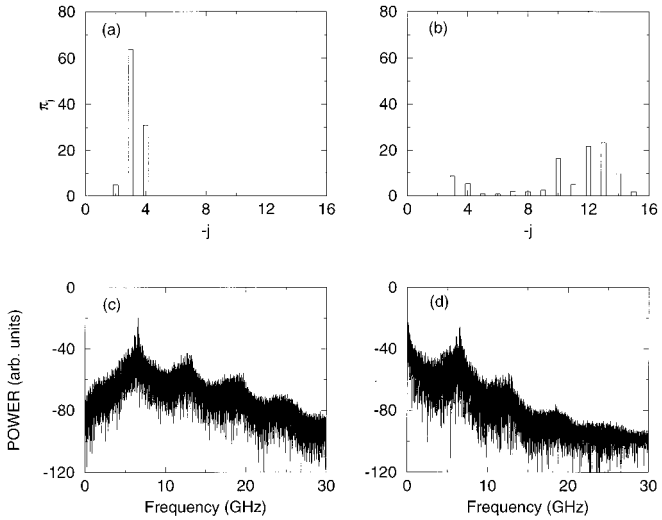

FIG. 2. Normalized scalograms of (a) $I(t)/I_{\rm sol}$ and (b) $\Delta(t)$. Simulated power spectra of the stationary signals of (c) $I(t)/I_{\rm sol}$ and (d) $\Delta(t)$.

The normalized scalogram of the time series of $\Delta(t)$ [shown in Fig. 2 (b)] is clearly different. Although the wavelet bands $j=-3$ and $j=-4$ carry some energy, the major part of it is concentrated in the low wavelet bands $j\leqslant -10$ (they represent the signal frequencies $f\leqslant f_{\rm ext}=0.1$ GHz). As we will show below, the differences between the two scalograms originate in the jumps between ECM's, which are clearly distinguished in the time evolution of $\Delta(t)$ while they cannot be resolved in the time evolution of $I(t)/I_{\rm sol}$. Notice that in the power spectra of the stationary signals [shown in Figs. 2(c) and 2(d)] one can recognize the same phenomenon; i.e., the low frequencies are more relevant in the spectra of $\Delta(t)$ than in the spectra of $I(t)/I_{\rm sol}$.

By sliding a 512-data-set window along the time series of $\Delta(t)$, we can study the time evolution of the energy distribution in the wavelet bands. Also, from the time evolution of π_j we can calculate the information cost function (ICF or $F_{\rm IC}$) [8], which is the information associated with the energy distribution in the wavelet bands, i.e.,

$$F_{\rm IC}=-\sum_j \pi_j \ln \pi_j. \tag{8}$$

Since the normalized scalogram can be thought as a probability distribution, the ICF is an easy to calculate entropy-like function that quantifies the degree of disorder of the transient dynamics. The time evolution of π_j is shown in

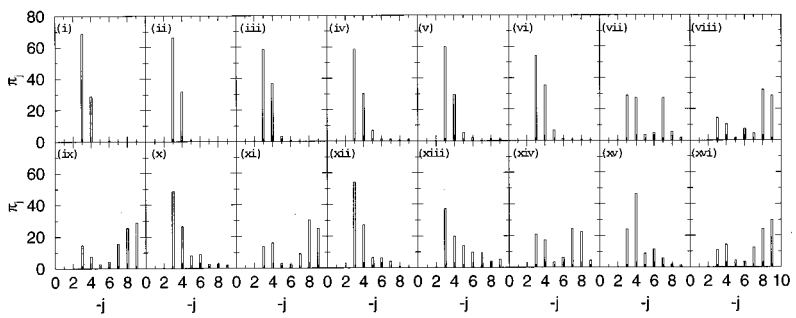

FIG. 3. Time evolution of the energy distribution, calculated from the time series of Fig. 1(b). The labels of the figures correspond to the labels in the Fig. 1(c).

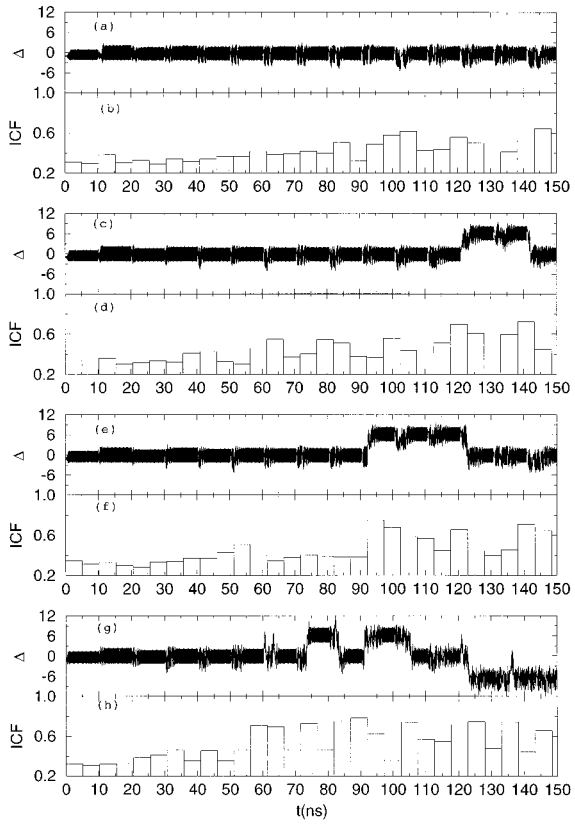

FIG. 4. Time evolution of the phase delay Δ and the ICF coefficient, for four increasing feedback levels. (a), (b) $\gamma = 3.15$ GHz; (c), (d) $\gamma = 3.50$ GHz; (e), (f) $\gamma = 3.85$ GHz; (g), (h) $\gamma = 4.80$ GHz.

Fig. 3, while the corresponding time evolution of the ICF is shown in Fig. 1(c). In the first stage of the transient dynamics (when the laser remains in the vicinity of the solitary laser mode), the energy is concentrated in two wavelet bands ($j = -3$ and $j = -4$). Figures 3(i)–3(vi) correspond to this period. This result trivially indicates that initially the oscillations are the typical relaxation oscillations. In the second stage of the transient dynamics, when the laser jumps between the attractors originating from the ECM's, the energy is distributed into a larger number of wavelet bands, indicating that more frequencies became involved in the dynamics. At the time of the transition from one attractor to another there is an abrupt energy transference to the low wavelet bands [Figs. 3(vii), 3(viii), 3(ix), 3(xi), 3(xiv), and 3(xvi) are calculated in time intervals in which a transition occurs].

In Fig. 4 we show the time series of $\Delta(t)$ and the corresponding time evolution of the ICF coefficient, for four increasing feedback levels, all above the onset of coherence collapse (they correspond to the feedback levels employed in Fig. 4 of Ref. [13] to reproduce the observed laser visibility).

Figure 4 demonstrates that the ICF provides a good measure of the degree of disorder of the transient dynamics. Notice that before the first jump (when the laser remains in the vicinity of the solitary laser mode) the ICF is approximately constant, although it suffers fluctuations that correspond to the bursts of irregular oscillations. In the second stage of the transient dynamics the ICF suffers important fluctuations; it increases when a jump occurs, and it decreases when the laser operates in a single attractor. However, its mean value increases with respect to the value in the first stage, indicating a more chaotic dynamics.

IV. CONCLUSIONS

In conclusion, we have shown that wavelet analysis is a powerful technique to study the destabilization process of a single-mode laser diode with optical feedback. We found an oscillatory approach to the coherence-collapsed state which consists of two stages. In the first stage the laser remains in the vicinity of the solitary laser mode, and the oscillations are initially the undamped relaxation oscillations. The WT shows that in this stage the energy is concentrated in the wavelet band that contains f_{ro}. As time passes the energy is slowly transferred toward the neighboring wavelet bands, indicating that new frequencies appear in the dynamics.

In the second stage of the evolution the laser jumps between the chaotic attractors introduced by the ECM's, and the WT shows that at the time of the jump there is a brusque energy transference to the very low wavelet bands. This phenomenon is reminiscent of the low frequency fluctuations (LFF's) that occur when the laser subjected to moderate feedback is biased near threshold. In this case the time evolution of the light intensity exhibits intermittent drops which in the frequency domain manifest themselves as LFF's at frequencies less than $f_{\mathrm{ext}}/10$. The LFF's have been attributed in the literature to a number of possible causes. Our results seem to be consistent with previous studies [1,15,16] that suggest that the LFF's are caused by a switching between destabilized ECM's.

It was also demonstrated that the information associated with the energy distribution in the wavelet bands (ICF) is a good way of quantifying the degree of disorder in the transient dynamics. We found that in the first stage of the evolution the ICF is approximately constant, although it shows fluctuations that indicate that during the destabilization process the laser undergoes intervals of regular and irregular behavior. In the second stage of the evolution the ICF shows large fluctuations; it increases at the time of the jump, and it decreases in the time intervals when the laser operates in a single state. Nevertheless, the mean value of the ICF increases with respect to the first stage, indicating a more chaotic dynamics.

The Lang-Kobayashi model is an approximate model, since it supposes that the field is uniform inside the laser cavity, that the forward and backward fields are equal, and that the grating and transverse effects can be neglected. Therefore, one might expect that the transient dynamics analyzed here may be very different from a real transient obtained experimentally with a real diode. However, this model has been successfully applied to the study of the transient dynamics of the laser (see, e.g., Ref. [17]) and therefore we expect our results be quite general in the transient regime to coherence collapse.

ACKNOWLEDGMENTS

This work was partially supported by the Project No. 47 of the BID-CONICyT, the Comision Sectorial de Investigacion Cientifica (CSIC), the PEDECIBA (Uruguay), and the CONICET (Argentina).

[1] T. Sano, Phys. Rev. A **50**, 2719 (1994).
[2] R. W. Tkach and A. R. Chraplyvy, IEEE J. Lightwave Technol. **LT-4**, 1655 (1986).
[3] J. Mörk and B. Tromborg, IEEE Photon. Technol. Lett. **2**, 21 (1990).
[4] J. Mörk, J. Mark, and B. Tromborg, Phys. Rev. Lett. **65**, 1999 (1990).
[5] A. Ritter and H. Haug, J. Opt. Soc. Am. B **10**, 130 (1993); **10**, 145 (1993).
[6] C. Masoller, Phys. Rev. A **50**, 2569 (1994).
[7] I. Daubechies, *Ten Lectures on Wavelets* (SIAM, Philadelphia, 1992).
[8] Y. Meyer, *Wavelet Alghoritms and Applications* (SIAM, Philadelphia, 1992).
[9] C. Chui, *An Introduction to Wavelets* (Academic Press, San Diego, 1992).
[10] R. Lang and K. Kobayashi, IEEE J. Quantum Electron. **QE-16**, 347 (1980).
[11] B. Tromborg, J. H. Osmundsen, and H. Olesen, IEEE J. Quantum Electron. **QE-20**, 1023 (1984)
[12] J. Mörk, B. Tromborg, and J. Mark, IEEE J. Quantum Electron. **QE-28**, 93 (1992).
[13] C. Masoller, C. Cabeza, and A. C. Sicardi, IEEE J. Quantum Electron. **QE-31**, 1022 (1995).
[14] L. Hudgins, C. A. Friehe, and M. E. Mayer, Phys. Rev. Lett. **71**, 3279 (1993).
[15] J. Mörk, B. Tromborg, and P. L. Christiansen, IEEE J. Quantum Electron. **QE-24**, 123 (1988).
[16] G. H. M. van Tarwijk, A. M. Levine, and D. Lenstra, IEEE J. Select. Topics Quantum Electron. **1**, 466 (1995).
[17] J. Dellunde, M. C. Torrent, C. R. Mirasso, E. Hernandez-Garcia, and J. M. Sancho, Opt. Commun. **115**, 523 (1995).